Journal of Astronomical Instrumentation, Vol. 10, No. 2 (2021) 2150008 (10 pages)

DOI: 10.1142/S2251171721500082

World Scientific
www.worldscientific.com

# Mid-Infrared Detector Array Technologies for *SOFIA* and Sub-Orbital Observatory Instruments

Judith L. Pipher[1,3], Craig W. McMurtry[1], Mario S. Cabrera[1,2] and William J. Forrest[1]

[1]Department of Physics and Astronomy
University of Rochester, Rochester NY 14627, USA

[2]Conceptual Analytics LLC
8209 Woburn Abbey Road
Glenn Dale, MD 20769, USA

[3]jlpipher@pas.rochester.edu

*Received February 1, 2021; Revised April 15, 2021; Accepted April 22, 2021; Published May 26, 2021*

The status of various photovoltaic, photoconductive, BIB/IBC, superlattice, TES and KID technologies to produce arrays sensitive from 15 to 50+ $\mu$m (Mid-infrared) will be reviewed to assess where reasonable investments should be made for *SOFIA* and other sub-orbital observatory instruments. These include HgCdTe, Si:As IBC, Si:Sb BIB, Ge:Ga, type 2 superlattice arrays of both III–V and II–VI materials and both TES and KID arrays. KID technologies for this wavelength region show promise, although to date there are no published experimental data on KID arrays for the mid-infrared.

*Keywords*: Mid-infrared; detector arrays; SOFIA; sub-orbital missions.

## 1. Introduction

The mid-region of the IR spectrum (15 to $\sim$50 $\mu$m) has seen far less concentrated detector development than at Short Wave IR (SWIR, $<$2.5 $\mu$m cutoff), Mid Wave IR (MWIR, $\sim$5 $\mu$m cutoff), Long Wave IR (LWIR, $\sim$14 $\mu$m cutoff), Very Long Wave IR (VLWIR, $>$14 $\mu$m cutoff, overlapping the short end of the Mid-IR band) and at far-IR/submillimeter wavelengths ($>$50 $\mu$m cutoff), where photodetector and bolometer developments have been optimized for sub-orbital and space astronomy, and even for ground-based astronomy where the Earth's atmosphere permits. Yet, strong continuum radiation from dust, as well as key diagnostic features from PAHs and silicate dust (e.g. Peeters *et al.*, 2002), MgS (Forrest *et al.*, 1981) and Buckminster Fullerene/C60 (Palotas *et al.*, 2020), and line emission from a variety of diagnostic molecules, atoms and ions fall within this wavelength range (Peeters *et al.*, 2002). We review here the current status of detector array development for this mid-region of the IR spectrum. This review builds on a presentation by one of us for the *SOFIA* Science Center Workshop: *Building the 2020–2025 Instrument Roadmap* (https://www.sofia.usra.edu/science/instruments/instrument-development/workshop-building-2020-2025-instrument-roadmap).

We will first explore the status of HgCdTe photovoltaic detector arrays, which have been successfully demonstrated at wavelengths from $<$1 to 16.7 $\mu$m. Extension to longer wavelengths has been proposed, and attempted to slightly longer than 17 $\mu$m, but to date has not been particularly successful, although there has been only very limited effort. One attempt involved forming a Type 2 superlattice (T2SL) HgTe/HgCdTe detector (Zhou *et al.*, 2002, 2003a,b). Other T2SL arrays, comprised of compounds formed from elements from the III–V groups from the periodic table, rather than from II–VI group materials, with 30+ $\mu$m design cutoff wavelengths have been attempted, but have not met their promise to date.

Si:As Blocked Impurity Band (BIB) or Impurity Band Conduction (IBC) arrays (5–28 $\mu$m) were

developed for *Spitzer Space Telescope's* IRS and IRAC instruments (from vendors Leonardo DRS and Raytheon Vision Systems, respectively), were later used in *WISE*, and *SOFIA* has utilized them in the FORCAST instrument. They are also used in the MIMIZUKU instrument on the Tokyo Atacama Observatory (TAO) 6.5-m telescope. Development of Si:As IBC arrays for *JWST's* MIRI instrument has led to excellent performance (Bright *et al.*, 2016). Si:As IBC arrays are extremely well-developed and mature as a consequence for low background use such as for *Spitzer* and *JWST*, but at higher backgrounds such as for *SOFIA* and ground-based telescopes, low frequency noise limits their performance.

Si:Sb BIB arrays (25–40 $\mu$m cutoff) were developed for *Spitzer's* IRS instrument by DRS, and have been also used in *SOFIA* FORCAST and the TAO 6.5 m telescope's instrument MIMIZUKU. Larger format arrays had been specified for the proposed *SPICA* mission, which as of 10/15/20 is no longer considered a candidate for the upcoming selection as ESA's 5th medium class mission in its *Cosmic Vision* Program. Si:Sb technology has mainly lapsed and requires re-development.

Ge:Ga photo-conductive arrays, sensitive from 40 to 120 $\mu$m when unstressed, have been used in *Herschel* PACS, *Spitzer* MIPS, and *SOFIA* FIFI-LS among other instruments: those are relatively small, individually built arrays. Much later, several authors began monolithic Ge:Ga array development for *AKARI* and *SPICA* (Fujiwara *et al.*, 2003; Kamiya *et al.*, 2010; Shirahata *et al.*, 2010). Ge:Ga BIB array development was once considered to be promising for astronomy (Watson *et al.*, 1993). Later efforts by Olsen *et al.* (1997; Ge:Sb BIB detectors) and Hanaoka *et al.* (2016; Ge:Ga BIBs) demonstrate longer wavelength cutoffs than conventional Ge:Ga arrays. The Ge:Ga BIBs exhibited degraded performance at the short wavelength side. While efforts to perfect the technology continue, Ge BIB technology remains immature.

Microwave Kinetic Inductance Detector (MKID) is a technology that is capable of photon counting and simultaneously energy resolving. Kinetic Inductance Detector Arrays (KIDs) have been developed for the visible/NIR (Lee *et al.*, 2020; Meeker *et al.*, 2018) and the Far-IR (Baselmans *et al.*, 2017; Ferrari *et al.*, 2018). It is hoped that KID arrays will perform well at Mid-IR wavelengths, but they have not yet demonstrated the required performance (Perido *et al.*, 2020), and to our knowledge, have not been included in any Mid-IR astronomical instrument to date. Transition Edge Superconductor (TES) arrays fabricated by the GSFC group have been demonstrated at the edge of the Mid-IR wavelength range in the *SOFIA* HAWC + instrument (the shortest wavelength Band A extends from 48.65 to 57.35 $\mu$m half power; Harper *et al.*, 2018). Audley *et al.* (2018) describe the development of $3 \times 49$ TES arrays fabricated by SRON for SAFARI (a *SPICA* instrument), with the shortest wavelength channel being 34–56 $\mu$m. There are not yet any published sensitivity measurements on this channel. Both KID and TES array development require substantial investment before they can be utilized for Mid IR astronomy. The recent cancellation of *SPICA* is a setback for European TES development.

## 2. Array Technologies Considered

### 2.1. *HgCdTe photovoltaic arrays*

$Hg_{1-x}Cd_xTe$ photovoltaic detectors can be tailored to different long wavelength cutoffs at a specific focal plane temperature, by modifying the Cd mole fraction $x$. This tailoring allows short wavelength, mid wavelength, as well as long wavelength sensitivity required for different astronomical purposes. The arrays can be matched to atmospheric transmission windows for ground-based astronomy, and mission specific purposes for space and sub-orbital missions. An example is the design of the proposed NASA mission *NEO Surveyor*, where 10 $\mu$m cutoff arrays are required to sense NEOs (Near Earth Objects) which have a temperature $\sim 300$ K. The empirically derived bandgap energy $E_g$ in eV as a function of $x$ and temperature $T$ is given by Hansen and Schmidt (1983):

$$E_g = -0.302 + 1.93x - 0.81x^2 + 0.832x^3 + 5.35(1 - 2x)10^{-4}T. \quad (1)$$

SWIR and MWIR HgCdTe arrays are extremely mature and have been demonstrated on a variety of telescopes, both in space and on the ground (e.g. Rauscher *et al.*, 2014). LWIR and VLWIR arrays are at a different point in their development. Our group at the University of Rochester has been working on LWIR arrays for several decades, and VLWIR arrays for about a decade (Bacon *et al.*, 2003, 2004, 2010; McMurtry *et al.*, 2013, 2016; Dorn

*et al.*, 2016, 2018; Cabrera, 2019; Cabrera *et al.*, 2020).

Obviously, a compositional gradient in the array will affect the bandgap, and hence the cutoff wavelength of a given array $\lambda_{co} = hc/E_g$. At a temperature of 40 K, the $\approx 10\,\mu$m cutoff arrays we at the University of Rochester have developed with JPL, University of Arizona and Teledyne Imaging Sensors for the proposed Near Earth Object survey mission (*NEO Surveyor*) perform extremely well (McMurtry *et al.*, 2013; Dorn *et al.*, 2016, 2018): they have a Cd fraction of $x = 0.232$ at this temperature. The crossover composition is at $x \approx 0.16$ where $E_g$ becomes 0 and the semiconductor changes into a semimetal (see Fig. 1 for $x$ ranging from 0.16 to 0.232). The closer $x$ approaches the crossover composition, the longer the cutoff wavelength of the semiconductor.

What are the longest cutoff wavelengths for HgCdTe projected before that transition occurs? Norton (2002) suggests 25 $\mu$m, while Betz and Boreiko (2001) project that wavelengths as long as 150 $\mu$m are possible at low focal plane temperatures, although they point out that either heterodyne or super-lattice techniques utilizing HgCdTe or HgTe and CdTe may prove to be more successful. As discussed below, some groups used long wave ($\approx 20\,\mu$m) HgCdTe as a photo-mixer for heterodyne detection in the Far-IR and there were also efforts to develop type II–VI superlattices employing HgCdTe.

Practically speaking, Teledyne Imaging Sensors physicists Don Lee and Majid Zandian claim that by only changing the alloy composition, the long wavelength program that our group at the University of Rochester ran yielded their longest wavelength alloy device they have produced to date ($\lambda_{co} = 16.7\,\mu$m, $x = 0.205$; Cabrera, 2019; Cabrera *et al.*, 2020). In order to achieve the desired results of detector arrays with $\lambda_{co} > 15\,\mu$m on a 1 k × 1 k format, lot splits including wafers of varying properties were required (see Wu, 1997, Fig. 12). Our results for the 16.7 $\mu$m array H1RG-20302 are shown in Figs. 2 and 3. With 150 mV applied bias at a focal plane temperature of 23 K, the median dark current is 32 e−/s and the well depth 34 ke−. Measurements of process evaluation chips from the same wafer as H1RG-20302 indicated the responsive quantum efficiency over the 6–12 $\mu$m waveband was 83%. Assuming an artificially imposed requirement on the dark current of 200 e−/s (there is no mission projected to use this array and thus no requirement, but that is the NEO Surveyor required upper limit for the 10 $\mu$m array), 79% of the pixels met this specification. Detailed examination of the I–V and $I$–$T$ curves for long-wave arrays in this study showed that the dark current was dominated by quantum tunneling (trap-band and band-band) at low temperatures, even though design steps were taken to minimize the tunneling contribution. Quantum tunneling is a strong function of bias, and with the H1RG Multiplexer readouts, appreciable applied reverse bias is required to develop sufficient well depth. Lower temperatures than 23 K were not attempted because the HxRG multiplexers do not operate well at $T < 23$ K. Since the focal plane temperature required for reasonable thermal dark

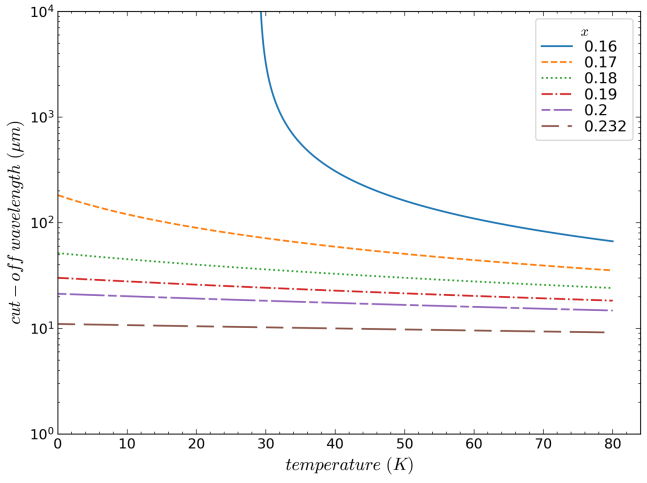


Fig. 1. Cut-off wavelength as a function of $T$ and Cadmium molar fraction $x$.

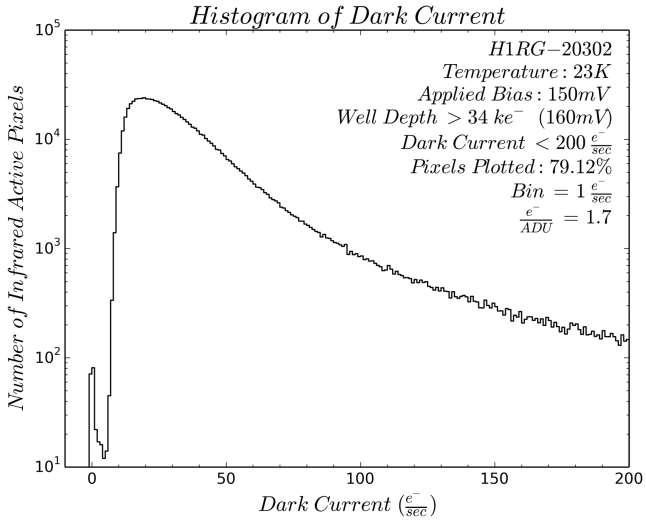


Fig. 2. Dark current histogram for H1RG-20302, a 16.7 $\mu$m cutoff HgCdTe array.

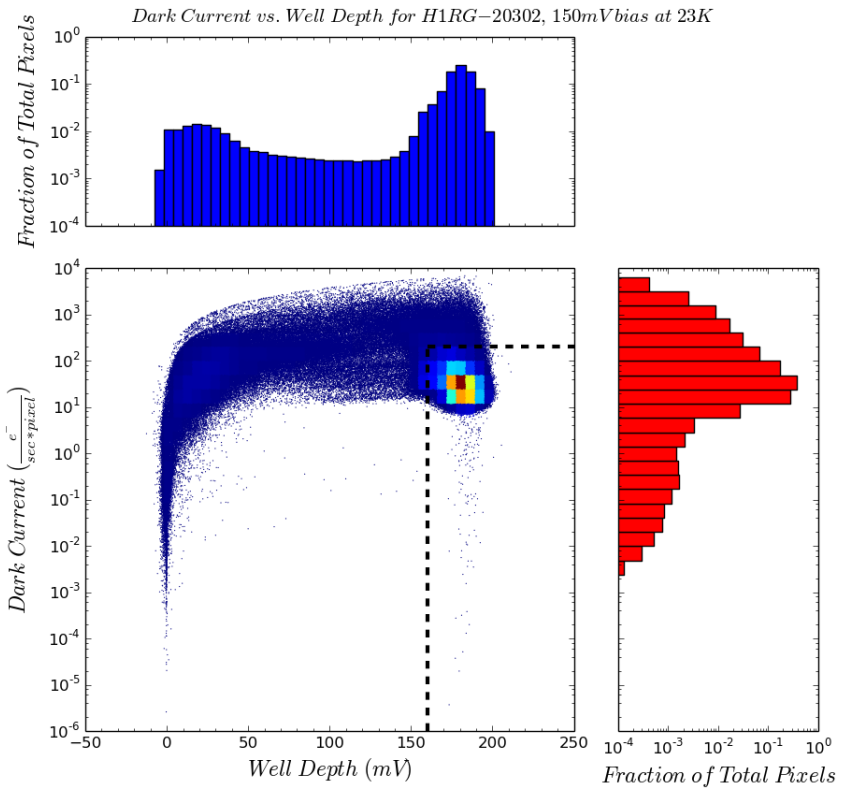


Fig. 3. Dark current versus well depth for H1RG-20302 a 16.7 $\mu$m HgCdTe array at $T = 23$ K.

currents decreases as the cutoff wavelength increases, new multiplexer designs are required which work at low temperatures. It is conceivable that $\lambda_{co} = 20+\,\mu$m alloy devices could be produced, but as the Hg fraction increases with longer cutoff wavelengths the arrays become softer and more prone to defects adversely affecting the dark current. In addition, control of the parameter $x$ across the array becomes more difficult. Phillips *et al.* (2002) cited difficulty in maintaining $\Delta x \leq \pm 0.002$ as required to maintain the wavelength within $\pm 0.5\,\mu$m at $14\,\mu$m. At $16.7\,\mu$m the issue is more difficult: $\Delta x \leq \pm 0.002$ corresponds to $\Delta\lambda \approx \pm 0.75\,\mu$m. So, as the wavelength continues to increase as the alloy composition $x$ is decreased, control of the wavelength becomes extremely challenging. An additional consideration for any scientific application in astronomy — the pixel pitch of the HxRG multiplexers is $18\,\mu$m: MTF requirements would necessitate a larger pixel pitch for these putative longer wavelength devices.

We have not had any $16.7\,\mu$m HgCdTe array material bonded to Teledyne's GEOSnap capacitive trans-impedance amplifier (CTIA) multiplexer readout: the CTIA readout does not require large applied reverse bias on the detector, reducing the effects of tunneling which plague detectors on traditional readouts. Other investigators (W. Hoffman and J. Leisenring (U. Arizona), M. Meyer (U. Michigan) and P. Hinz (SantaCruz)) have been investigating this multiplexer readout with shorter wave ($13\,\mu$m) HgCdTe material that our group developed on the road to producing the $16.7\,\mu$m device.

Spears (1983) reported developing wide-band HgCdTe photodiode photo-mixers at $28\,\mu$m for a laser heterodyne spectrometer. The devices exhibited strong band-band tunneling, and had low optical absorption coefficient at $\lambda = 28\,\mu$m. The donor concentration was less than $5 \times 10^{14}\,\mathrm{cm}^{-3}$, the diode diameter $100\,\mu$m, and the operating temperature was 20 K.

Later, Spears (1988) reported developing $20\,\mu$m photoconductor photo-mixers from LPE $p$-type $Hg_{0.812}Cd_{0.188}Te$ since photodiodes have limited wideband performance in the long wavelength IR because of tunneling. Photoconductors operate at much lower electric fields than photodiodes: Spears apparently never followed up on this development (it was far too difficult to control the alloy with liquid phase epitaxy and the performance garnered was modest). Although molecular beam epitaxy

(MBE) processes utilized today are more accurate, as noted above alloy composition control at the longer wavelengths remains challenging.

### 2.2. *Super-lattice devices*

In super-lattice devices, the bandgap is controlled by adjusting the thicknesses of alternating layers of suitable materials in a periodic fashion: these nanolayers are usually formed using molecular beam epitaxy. At 77 K, the bandgap of the semi-metal HgTe is −0.26 eV and the semi-conductor CdTe is 1.6 eV. Although II–VI materials can be utilized to form a superlattice (e.g. HgTe/CdTe or $Hg_{1-x}Cd_xTe/Cd_{1-y}Zn_yTe$), currently III–V materials such as InAs/InGaSb are more commonly used. Type II super-lattice detectors (T2SL), in which the band gaps of the two host semiconductors are in either a staggered or a broken-gap alignment (Sai-Halasz *et al.*, 1978), are the most common type super-lattice SL. In principle, SL detectors for the Mid-IR and Far-IR have advantages over alloy devices, since the cutoff wavelength is easier to control, depending primarily on the thickness of the wells, and since tunneling is expected to be far less of an issue. Betz and Boreiko worked with the University of Illinois Microphysics group (Zhou *et al.*, 2002, 2003a,b) on development of a HgTe/HgCdTe MBE superlattice, among others. This one, a 100 layer SL, was grown on CdZnTe substrate and a mid-wave IR HgCdTe buffer layer. The thickness of the HgTe wells was 80 Å and of the $Hg_{0.05}Cd_{0.95}Te$ barriers 77 Å producing a SL period of 157 Å. Then another buffer layer and a CdTe cap layer were grown. All layers were undoped: the absorption edge wavelength at 5 K is about 30 $\mu$m.

The authors investigated the effects of annealing on the SLs, since to form a diode to produce a useable detector, p-type material would be introduced through annealing. Unfortunately, interdiffusion of the wells and barriers resulted from the anneals, shifting the absorption edges to higher energies. A 300 $\mu$m × 300 $\mu$m single pixel photoconductive device was constructed and its spectral response at 77 K was measured — the cutoff wavelength was determined to exceed 20 $\mu$m, but since they used a ZnSe window on their dewar, they could not specify the actual cutoff wavelength.

At the Northwestern Center for Quantum Devices (CQD), Center Director Razeghi and colleagues (Razeghi *et al.*, 2006) reviewed progress made in using III–V materials in preference to II–VI materials (stronger covalent bonds, greater uniformity) to produce T2SLs. SLs with cutoff wavelengths ranging from 3.7 to as long as 32 $\mu$m (Wei *et al.*, 2002) were grown to produce InAs/GaSb photodiodes. Brown *et al.* (2003) developed p-i-n diodes of InAs/GaSb and InAs/InGaSb with $\lambda_{co} > 22\,\mu$m, and held out hope for good photodiodes out to 32 $\mu$m based on Wei *et al.* More recent work at CQD has concentrated on high temperature MWIR/LWIR devices (HOT arrays), and although they developed 1 k × 1 k arrays, they were not appropriate for astronomy, even for the higher background ground-based telescopes.

Daumer *et al.* (2019) reviewed the state-of-the-art European HgCdTe arrays ($\lambda < 14\,\mu$m) as compared to III–V T2SL arrays, and concluded that while the T2SLs potentially have more promise in terms of scalability, stability, and Auger dark current, they have not yet met their promise. Rogalski *et al.* (2019) also reviewed T2SL arrays in comparison with alloy arrays such as HgCdTe. From these recent reviews, it seems clear that T2SL arrays have not yet been successfully developed for space or sub-orbital application. Current emphasis appears to be on HOT detector arrays, while cryogenically cooled arrays are required for most space and sub-orbital astrophysics, even at the higher backgrounds of *SOFIA*.

### 2.3. *Si:As and Si:Sb arrays*

Si:As BIB arrays with $\lambda_{co} = 28\,\mu$m were originally invented by Petroff and Stapelbroek (1986) at Rockwell International Corporation, later Leonardo DRS. The *Spitzer Space Telescope* IRS and MIPS instruments included 128 × 128 format devices (Van Cleve *et al.*, 1995; Hora *et al.*, 2004), and future larger format generations of these devices flew on *WISE* (Mainzer *et al.*, 2008) and *SOFIA* FORCAST (Herter *et al.*, 2012). Si:As IBC 256 × 256 arrays, developed by Raytheon Vision Systems — were included as the 2 longer wave channels of the *Spitzer* IRAC instrument (Hora *et al.*, 2004). These arrays in 1024 × 1024 format have continued to be further developed for the *JWST* MIRI experiment (Rieke *et al.*, 2015) and for the MIMIZUKU instrument on the TAO 6.5-m telescope (Kamizuka *et al.*, 2012). Si:As BIB/IBC arrays represent a mature technology for Mid-IR wavelengths to 28 $\mu$m for low background applications.

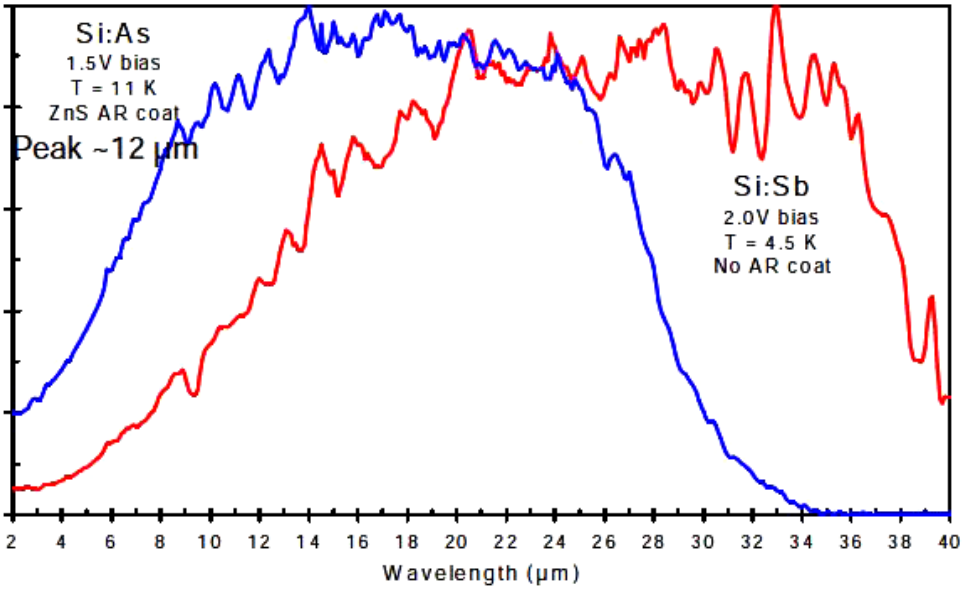


Fig. 4. Relative spectral response of low background DRS Si:As and Si:Sb BIB arrays (reproduced by permission: Khalap & Hogue, 2012).

Si:Sb BIB arrays, with wavelength response to $\lambda_{co} = 40\,\mu$m (Fig. 4), have only been developed by Rockwell/DRS, originally for the *Spitzer* IRS experiment and for *SOFIA* FORCAST, in relatively small formats. The technology was sufficiently mature in 2012 that $128 \times 128$ arrays had been tested for the high background TAO 6.5 m MIMIZUKU instrument development (Kamizuka *et al.*, 2012). The low background development for *SPICA* (Khalap & Hogue, 2012) demonstrated $1024 \times 1024$ arrays, although as noted, *SPICA* has now been canceled Originally, Hirokazu Kataza (JAXA) led the Si:Sb development for the *SPICA* Mid-IR camera and Spectrometer (Kataza *et al.*, 2015), but Takehiko Wada (JAXA) has taken over. *SPICA* was in Phase A development prior to cancellation.

Unfortunately, as Leonardo DRS puts it, the Si:Sb process is "stale" since the 2012 employees who worked on the project are no longer at DRS. A junior colleague had been taught the ropes, but DRS has not had sufficient financial incentive to begin the \$6–8M process of redevelopment. For $\lambda_{co} = 40\,\mu$m, Si:Sb is the most mature technology existing today. A more highly doped IR active layer would increase $40\,\mu$m response somewhat at the expense of increased dark current. The only *astronomically demonstrated* detector array technologies for $\lambda > 40\,\mu$m include smaller format stressed and unstressed Ge:Ga detector arrays and Transition Edge Sensor — TES arrays.

### 2.4. *Ge:Ga arrays*

Unstressed Ge:Ga arrays are sensitive from $< 40$–$120\,\mu$m (Young *et al.*, 1998). Very small Ge:Ga arrays were developed for the *Kuiper Airborne Observatory's* FIFI experiment (Stacey *et al.*, 1992) and Young *et al.* (1998) developed non-monolithic arrays for *Spitzer* MIPS by stacking $1 \times 32$ linear modules. Based on earlier *Herschel* PACS arrays, Rosenthal *et al.* (2000) described development of $16 \times 25$ photoconductor arrays of unstressed Ge:Ga for *SOFIA* FIFI-LS, as well as stressed Ge:Ga for wavelengths beyond 120 $\mu$m. Two dimensional direct monolithic Ge:Ga arrays (Fig. 5) were in development for *SPICA* (Shirahata *et al.*, 2010; Kamiya *et al.*, 2010) based on very small $3 \times 20$ monolithic arrays successfully flown on *AKARI* described below.

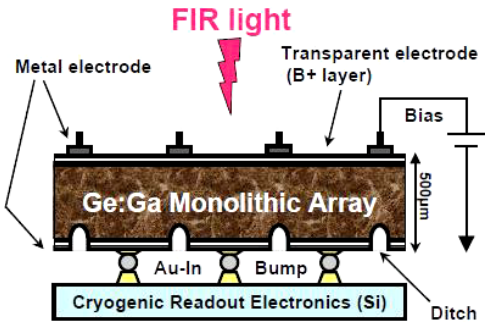


Fig. 5. Structure of planned $64 \times 64$ SPICA Ge:Ga array. Reproduced by permission from Shirahata *et al.* (2010).

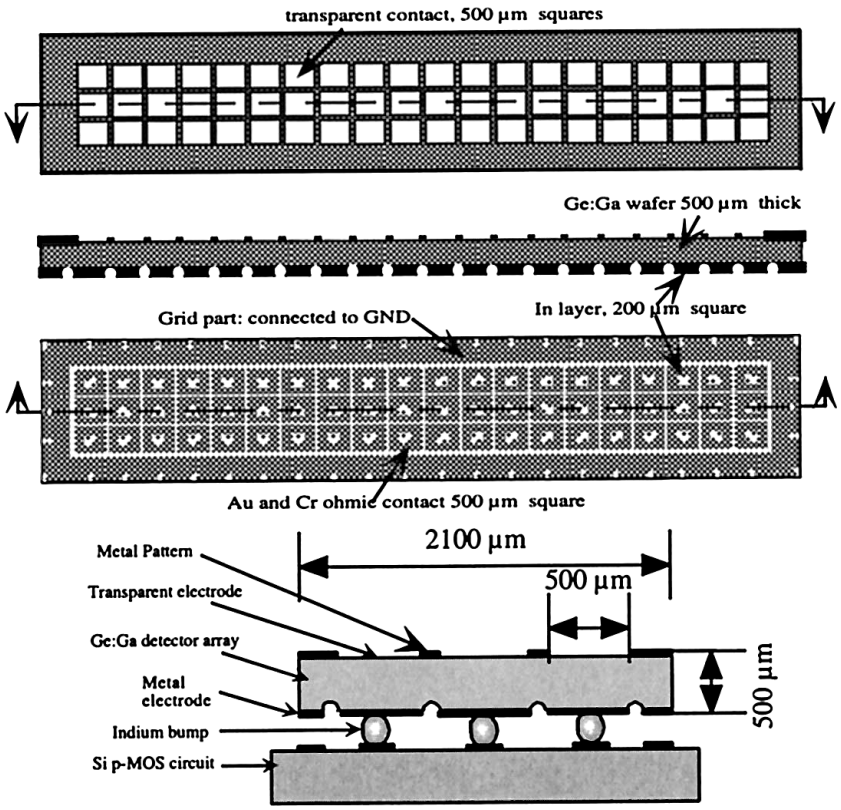


Fig. 6. First monolithic Ge:Ga array flown on *AKARI*. Reprinted with permission from Fujiwara *et al.* (2003), ©The Optical Society.

This first monolithic 2D Ge:Ga array for Astronomy was flown in 2006 on *AKARI* or ASTRO-F (Fujiwara *et al.*, 2003) and is shown in Fig. 6. The development of monolithic arrays was a big step forward to making these devices practical for the future. The arrays, however, are considerably more complex to produce than the shorter mid-IR wavelength HgCdTe and Si:As/Sb arrays described earlier. The quantum efficiency of a free-standing Ge:Ga photoconductor is low. In order to enhance the absorption of radiation, the non-monolithic devices may be enclosed in individual gold-plated cavities, with area-filling light cones, or in the case of the *Spitzer* devices, solid Ge feed horns. Of course, the monolithic arrays cannot be enclosed in cavities. As Beeman and Haller (1994) first showed, contacting each non-cavity pixel in the longitudinal direction yielded the best performance, and most of the arrays make use of that configuration. For the small *AKARI* array (Fig. 6), $B^+$ implants form the transparent electrodes and metallic stripes on the transparent electrode define the pixels. Indium bumps between the detectors and the specially designed three-step differential CTIA p-Si MOS readout form the detector array. In order to increase responsivity, a BIB-like structure on the array was implemented. Earlier Ge:Ga BIB attempts (e.g. Watson *et al.*, 1993) were only partially successful.

As noted above, Kamiya *et al.* (2010) and Shirahata *et al.* (2010) were developing a larger $64 \times 64$ fully monolithic Ge:Ga array for the now cancelled *SPICA*. The transparent electrode on the top layer is formed by $B^+$ implants, and the pixels are separated by $50\,\mu$m wide, $30\,\mu$m deep grid-shaped ditches on the back surface. Au bumping technology was developed and utilized, and a number of other technological advances were required, including AR coating. Prototype $5 \times 5$ array measurements were encouraging.

### 2.5. *KID and TES arrays*

Perido *et al.* (2020) describe extending the Kinetic Inductance Detector (KID) technology to the mid-IR for future space and sub-orbital observatories. (Jason Glenn described that development at the *SOFIA* Workshop referenced above). Their goals are ambitious — to extend the wavelength range of existing sensitive aluminum KIDs for the proposed mission concept "Galaxy Evolution Probe" to

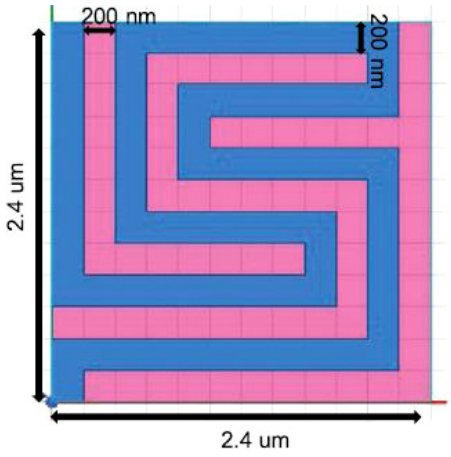


Fig. 7. Inductor portion of a 10 $\mu$m KID unit cell repeated over the entire absorber area (Perido *et al.*, 2020). Open source article published under terms of Creative Commons Attribution International License 4.0 (CC-BY).

encompass 10–100 $\mu$m wavelengths, as well as the already existing and well developed 100–400 $\mu$m technology. The detector element is an inductor as shown in Fig. 7. Perido *et al.* (2020) have designed aluminum KIDs on Si and Ge substrates with simulated absorption efficiencies of 73–80%. Their first test device exhibited noise caused by switching dipoles in the substrate which caused altered capacitance. They calculate the theoretical NEP to be $10^{-17}$ W/$\sqrt{\text{Hz}}$ including all noise sources, but only estimate the quasiparticle lifetime. The absorption can be shifted in wavelength by tuning the aluminum line widths and the unit cell sizes. The group plans to develop a 30 $\mu$m wavelength device next, and to investigate AR coatings and the addition of a microlens array to improve sensitivity.

Antenna coupled MKID arrays for submm range astrophysics have been developed by SRON (Ferrari *et al.*, 2018) and current efforts are directed to extending this technology to 30 $\mu$m.

TES arrays for the mid-IR are somewhat more advanced developmentally than MKIDs: for example they are currently used in the HAWC+ camera (Harper *et al.*, 2018). SOFIA Observer's Handbook, cycle 9 update (https://www.sofia.usra.edu/science/proposing-and-observing/observers-handbook-cycle-9/7-hawc) describes the TES arrays used in HAWC+, with absorbing coatings optimized across the 50–240 $\mu$m bandpass (Band A extends from 48.65 to 57.35 $\mu$m HPBW and exhibits approximately 50% operability). The two $32 \times 40$ imaging sub-arrays (Fig. 8), with pixels of size 1.135 mm square (Jhabvala *et al.*, 2014) are each suspended within a supporting frame and are cooled to 0.1–0.2 K (Harper *et al.*, 2018).

The *Origins* Space Telescope Technology Plan (2019) describes further development of TES technology in the mid-IR to improve the NEP, increase the format, and characterize the stability for consideration for the proposed *Origins* Space Telescope spectrometer experiment, MISC. Alternate technologies (HgCdTe, Si:AS IBC) are also being evaluated for MISC (Roellig *et al.*, 2020).

## 3. Summary

Mid-IR 15-50+ $\mu$m detector array strategies are in various phases of development. Some technologies are relatively mature: others are at the cusp of

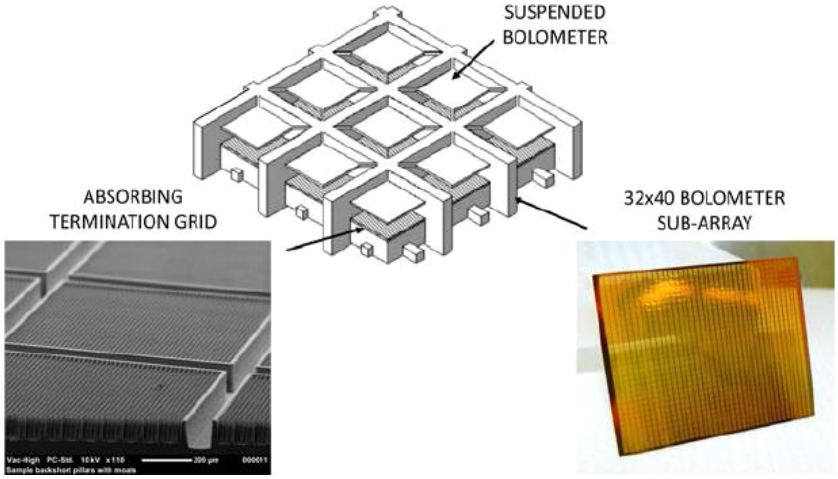


Fig. 8. Backshort Under Grid design of *SOFIA* TES arrays (Harper *et al.*, 2018). Open source article published by World Scientific Publishing Company, distributed under terms of Creative Commons Attribution 4.0 (CC-BY).

tantalizing success. The *Origins* Space Telescope Technology Plan (2019) includes parallel development of TES, HgCdTe and Si:As IBC Mid-IR arrays for the MISC experiment, with the extremely difficult task of exhibiting 5 ppm stability for a very sensitive, large format array (Roellig *et al.*, 2020). It seems likely that the KID arrays will also prove competitive in the Mid-IR, if sufficient funding continues. Since current emphasis on Type 2 super lattice (T2SL) arrays extends primarily to high temperature operation, it is unlikely that they will prove competitive for space and sub-orbital astrophysics by 2030. Since *SPICA*, the ESA/JAXA mission with a far infrared telescope was cancelled, Si:Sb array development is unlikely to receive sufficient funding to advance, unless NASA or ESA considers its viability for future missions crucial.

## References


Audley, M., de Lange, G., Gao, J.-R. *et al.* [2018] *Proc. SPIE* **10708**, 107080K.

Bacon, C. M., Pipher, J. L., Forrest, W. J. *et al.* [2003] *Proc. SPIE* **4850**, 927B.

Bacon, C. M., McMurtry, C. W., Pipher, J. L. *et al.* [2004] *Proc. SPIE* **5167**, 313.

Bacon, C. M., McMurtry, C. W., Pipher, J. L. *et al.* [2010] *Proc. SPIE* **7742**, 77421U.

Baselmans, J. J. A., Bueno, J., Yates, S. J. C. *et al.* [2017] *A&A* **601**, A89.

Beeman, J. W. & Haller, E. E. [1994] *Infrared Phys. Technol.* **35**, 827.

Betz, A. L. & Boreiko, R. T. [2001] *Proc. SPIE* **4454**, 1.

Bright, S. N., Ressler, M. E., Alberts, S. *et al.* [2016] *Proc. SPIE* **9904**, 41.

Brown, G. J., Houston, S., Szmulowicz, F. *et al.* [2003] *Proc. SPIE* **5074**, 191.

Cabrera, M. [2019] *Development of 15 μm Cutoff Wavelength HgCdTe Detector Arrays for Astronomy*, PhD Thesis, University of Rochester.

Cabrera, M. S., McMurtry, C. M., Forrest, W. J. *et al.* [2020] *J. Astron. Telesc. Instrum. Syst.* **6**, 011004.

Daumer, V., Rutz, F., Wörl, A. *et al.* [2019] *Proc. SPIE* **11180**, 111806J.

Dorn, M., Pipher, J. L., McMurtry, C. *et al.* [2016] *J. Astron. Telesc. Instrum. Syst.* **2**, 036002.

Dorn, M., McMurtry, C., Pipher, J. L. *et al.* [2018] *Proc. SPIE* **10709**, 1070907.

Ferrari, L. *et al.* [2018] *IEEE Trans. Terahertz Sci. Technol.* **8**, 127.

Forrest, W., Houck, J. & McCarthy, J. [1981] *Astrophys. J.* **248**, 195.

Fujiwara, M., Hirao, T., Kawada, M. *et al.* [2003] *Appl. Opt.* **42**, 2166.

Hanaoka, M., Kaneda, H., Oyabu, S. *et al.* [2016] *J. Low Temp. Phys.* **184**, 225.

Hansen, G. L. & Schmidt, J. L. [1983] *J. Appl. Phys.* **54**, 1639.

Harper, D. A., Runyan, M., Dowell, D. *et al.* [2018] *J. Astron. Instrum.* **7**, 1840008.

Herter, T. L., Adams, J. D., DeBuizer, J. M. *et al.* [2012] *Astrophys. J.* **749**, L18.

Hora, J., Fazio, G., Allen, L. *et al.* [2004] *Proc. SPIE* **5548**, 77H.

Houck, J. R., Roellig, T. L., Van Cleve, J. *et al.* [2004] *Proc. SPIE* **5548**, 62H.

Jhabvala, C. A., Benford, D. J., Brekosky, R. P. *et al.* [2014] *Proc. SPIE* **9153**, 91533C.

Kamiya, S., Shirahata, M., Matsuura, S. *et al.* [2010] in *35th Int. Conf. Infrared, Millimeter, and Terahertz Waves*, Rome, pp. 1–2, doi: 10.1109/ICIMW.2010.5612466.

Kamizuka, T., Myata, T. & Sako, S. [2012] *Proc. SPIE* **8446**, 84466P.

Kataza, H., Sakon, I., Wada, T. *et al.* [2015] *J. Astron. Instrum.* **4**, 1550001.

Khalap, V. & Hogue, H. [2012] *Proc. SPIE* **8512**, 81520O.

Lee, K., Choi, J., Genova- Santos, R. T. *et al.* [2020] *J. Low Temp. Phys.* **200**, 384.

Mainzer, A., Larsen, M., Stapelbroek, M. G. *et al.* [2008] *Proc. SPIE* **7021**, 70210X.

McMurtry, C., Lee, D., Beletic, J. *et al.* [2013] *Opt. Eng.* **52**, 091804-8.

McMurtry, C. W., Dorn, M., Cabrera, M. *et al.* [2016] *Proc. SPIE* **9915**, 99150D.

Meeker, S. R., Mazin, B. A., Walter, A. B. *et al.* [2018] *Publ. Astron. Soc. Pac.* **130**, 65001.

Norton, P. [2002] *Opto-Electron. Rev.* **10**, 159.

Olsen, C., Beeman, J. & Haller, E. [1997] *Proc. SPIE* **3122**, 348.

Origins Space Telescope Technology Plan [2019] https://asd.gsfc.nasa.gov/firs/docs/.

Palotás, J., Martens, J., Berden, G. & Oomens, J. [2020] *Nat. Astron.* **4**, 240.

Perido, J., Glenn, J., Day, P. *et al.* [2020] *J. Low Temp. Phys.* **199**, 696.

Peeters, E. *et al.* [2002] *A&A* **381**, 571.

Petroff, M. D. & Stapelbroek, M. G. [1986] United States Patent 4,568,960.

Phillips, J. D., Edwall, D. D. & Lee, D. L. [2002] *J. Electron. Mater.* **31**, 664.

Rauscher, B. J., Boehm, N., Cagiano, S. *et al.* [2014] *Publ. Astron. Soc. Pac.* **126**, 739.

Razeghi, M., Wei, Y., Hood, D. *et al.* [2006] *Proc. SPIE* **6206**, 62060N.

Rieke, G. H., Ressler, M. E., Morrison, J. E. *et al.* [2015] *Publ. Astron. Soc. Pac.* **127**, 665.

Roellig, T. L., McMurtry, C., Greene, T. *et al.* [2020] *J. Astron. Telesc. Instrum. Syst.* **6**(4), 041503.

Rogalski, A., Martyniuk, P. & Kopytko, M. [2019] *Prog. Quantum Opt.* **68**, 100228.

Rosenthal, D., Beeman, J. W., Geis, N. *et al.* [2000] *Proc. SPIE* **4014**, 156.

Sai-Halasz, G. A., Chang, L. L., Welter, J.-M. *et al.* [1978] *Solid State Commun.* **27**, 935.

Shirahata, M., Kamiya, S., Matsuura, S. *et al.* [2010] *Proc. SPIE* **7741**, 77410B.

Spears, D. L. [1983] *Proc. SPIE* **0300**, 174.

Spears, D. L. [1988] in *Proc. Conf. Lasers and Electro-Optics*, TUD-3.

Stacey, G. G., Beeman, J. E. & Haller, E. E. [1992] *Int. J. Infrared Millim. Waves* **13**, 1689.

Van Cleve, J. E., Herter, T. L., Buttrrini, R. *et al.* [1995] *Proc. SPIE* **2553**, 502V.

Watson, D. M., Guptill, M. T., Huffmann, J. E. *et al.* [1993] *J. Appl. Phys.* **74**, 4199.

Wei, Y., Gin, A., Razeghi, M. *et al.* [2002] *Appl. Phys. Lett.* **81**, 3675.

Wu, J. [1997] *Development of Infrared Detectors for Space Astronomy*, PhD Thesis, University of Rochester.

Young, E. T., Davis, J. T., Thompson, C. L. *et al.* [1998] *Proc. SPIE* **3354**, 57Y.

Zhou, Y. D., Becker, C. R., Ashokan, A. *et al.* [2002] *Proc. SPIE* **4795**, 121.

Zhou, Y. D., Becker, C. R., Selamet, Y. *et al.* [2003a] *J. El. Mat.* **32**, 608.

Zhou, Y. D., Zhao, J., Boreiko, R. *et al.* [2003b] *Proc. SPIE* **5209**, 100.